


Cite this: *J. Mater. Chem. C*, 2017,
5, 9370Received 1st July 2017,
Accepted 3rd August 2017

DOI: 10.1039/c7tc02953e

rsc.li/materials-c

Preparation and optoelectronic behaviours of novel electrochromic devices based on triphenylamine-containing ambipolar materials†

De-Cheng Huang,‡ Jung-Tsu Wu,‡ Yang-Ze Fan and Guey-Sheng Liou *

Two new triphenylamine-containing ambipolar electrochromic materials with ether linkages, 1-(2-(4-(bis(4-methoxyphenyl)amino)phenoxy)ethyl)-1'-ethyl-[4,4'-bipyridine]-1,1'-dium tetrafluoroborate (**TPA-Vio**) and 2-(4-(bis(4-methoxyphenyl)amino)phenoxy)anthracene-9,10-dione (**TPA-OAQ**), were successfully synthesized and fabricated into novel electrochromic devices. These devices demonstrated interesting and much higher performance than devices derived from **TPA-3OMe** with respect to driving voltage, switching time, and electrochromic stability.

Introduction

“Chromism” refers to colour changes within a material subjected to an external stimulus such as light, temperature, and electric field. Electrochromism can be recognized as the reversible colouration of a material in the UV-vis-NIR region associated with electrochemically induced oxidative and reductive states. Generally, common electrochromic (EC) materials can be classified into four different groups, namely inorganic coordination complexes, transition-metal oxides, conjugated polymers, and organic molecules.^{1,2} Electrochromic devices (ECDs) of active optical modules possess many advantages, such as high contrast, lower applied potential and power consumption, colour control, and bistable characteristics. In recent years, with increasing awareness of energy saving and carbon reduction, EC technology has gradually received more attention and could be applied to smart windows in construction, sunroof and anti-glare rear-view mirrors in vehicles, and electronic paper and displays. EC glass has mainly been based on inorganic metal oxides for several years, but cost is becoming a major problem in producing large quantities of these materials. Organic EC materials have become promising candidates due to showing various characteristics, including flexibility (necessary for flexible device fabrications), easy processing, high colouration efficiency, and multicolour properties, within the same material.

Triphenylamine (TPA) derivatives are famous for their marvellous photoactive and electroactive properties, and are representative alternatives for optoelectronic applications, including light-emitters, hole-transporters, and photovoltaic, EC, and memory devices.^{3,4} Our research group has reported a series of electroactive high-performance polymers based on TPA derivatives with respect to synthesis and characteristic evaluation.⁵ Furthermore, we have proposed a method to reduce the applied oxidation potential that could enhance the electrochemical stability, and investigated the EC colour-merging behaviour by designing different polymer structures and fabricating them into ECDs. Compared with polymeric EC materials, small organic molecules have merits such as fast mobility within the electrolyte, lower cost, and easily tunable EC properties *via* facile structural modifications. According to our related studies,⁶ TPA can readily lose an electron during electrochemical oxidation to produce stable radical cation with a discernible change in colour. Introducing electron-donating substituents to the *para*-position of phenyl groups in the TPA unit allows it to not only act as a protective group, preventing electrochemical oxidative coupling and affording stable cationic radicals, but also decrease the oxidation potential owing to its electron-donating ability, resulting in notably improved redox and EC reversibility of the obtained TPA-based materials.

Viologen derivatives are known as organic EC materials with distinct colouring performances due to the reversible optical colour change in reduction redox cycles. Under cathodic scanning, viologen undergoes reversible reduction from a dication to a monocation radical, producing a high-contrast variation in transmittance over the visible light region.^{7–9} Modifying the pendent substituents of viologen can tune the colour by adjusting different molecular energy levels. Moreover, anthraquinone derivatives have drawn attention as redox-active and near-infrared

Functional Polymeric Materials Laboratory, Institute of Polymer Science and Engineering, National Taiwan University, 1 Roosevelt Road, 4th Sec., Taipei 10617, Taiwan. E-mail: gsliau@ntu.edu.tw; Fax: +886-2-33665237; Tel: +886-2-33665315

† Electronic supplementary information (ESI) available: Measurement, synthesis of 1–4, NMR spectra of 5–7 and the electrochromic data of ECD based on **TPA-3OMe**. See DOI: 10.1039/c7tc02953e

‡ These authors contributed equally to this work.

(NIR) EC materials. Anthraquinone possesses strong electron-withdrawing characteristics and is usually used in bleaching pulp for papermaking and conjugated polymers as an electron acceptor unit.

Furthermore, anthraquinone derivatives are more interesting as cathodic EC materials because of their high electrochemical stability during reduction redox procedures.¹⁰ Generally, a single EC material is insufficient to achieve high contrast and full-band absorption in the visible light region. Therefore, collocating anodic and cathodic EC materials should be a judicious approach to obtaining complementary colours. Moreover, it could provide mutual charge-storage layers to enhance the response capability. In previous studies,^{11–14} Hsiao and our group have reported triarylamine-based ambipolar EC polymers (such as polyimides and polyamides), in which one polymer chain exhibits interesting EC behaviour with multicolour characteristics in both oxidized and reduced states. The resultant polymers possessed crucial properties, such as excellent thermal stability, high colouration efficiency (CE), notable quick switching time (response capability), and outstanding electroactive reversibility.

In 2017, Zhou *et al.* prepared solution-type electrochromic devices derived from ambipolar materials with electron-withdrawing benzodipyrrolidone moieties.¹⁵ Herein, we propose a facile “linkage” approach to merging ambipolar EC behaviours using a single small molecule. Two novel ambipolar EC materials, 1-(2-(4-(bis(4-methoxyphenyl)amino)phenoxy)ethyl)-1'-ethyl-[4,4'-bipyridine]-1,1'-dium tetrafluoroborate (**6**) and 2-(4-(bis(4-methoxyphenyl)amino)phenoxy)anthracene-9,10-dione (**7**), were synthesized, fully characterized, and then fabricated into the EC devices to evaluate their EC performance. With the “linkage” approach, the incorporation of counter EC moieties as charge-trapping layers into TPA units is expected to produce a two-colour combination, reduce the driving potential and switching time, and intensify EC reversibility.

Experimental

General considerations

TPA-3MeO was prepared using a similar method to that previously reported.¹⁶ Tetrabutylammonium tetrafluoroborate (TBABF₄) was prepared as follows: DI water containing tetrabutylammonium bromide (5.00 g) was added dropwise to a saturated NaBF₄ aqueous solution, producing the desired white precipitate, which was then directly recrystallized from hot water. The remaining reagents were received from commercial sources and used without further purification.

Material synthesis

4-(2-Bromoethoxy)-N,N-bis(4-methoxyphenyl)aniline (TPA-OBr) (5). A mixture of 4-(bis(4-methoxyphenyl)amino)phenol **4** (1.4 g, 5 mmol) was dissolved in 1,2-dibromoethane (20 mL, 227 mmol), and then potassium hydroxide solution (1.1 g, 20 mmol) containing tetrabutylammonium bromide (0.026 g, 0.08 mmol) was added dropwise and stirred at 90 °C for 24 h. After cooling to room temperature, water (100 mL) was added and the crude product

was extracted with CH₂Cl₂, condensed, and dried, to give 1.71 g (86% yield) of brown viscous liquid. Further purification by flash column chromatography (dichloromethane/hexane = 1 : 2) afforded the yellow liquid (78% final yield). ¹H NMR (400 MHz, DMSO-*d*₆, δ): 3.71 (s, 6H), 3.77 (t, 2H), 4.26 (t, 2H), 6.86 (m, 12H); ¹³C NMR (100 MHz, DMSO-*d*₆, δ): 31.76, 55.53, 68.42, 115.06, 115.93, 124.38, 125.06, 141.53, 153.40, 155.11; ESI-MS *m/z*: calcd for (C₂₂H₂₂BrNO₃)⁺, 427.08; found, 427.09. Anal. calcd for C₂₂H₂₂BrNO₃: C 57.74, H 4.99, N 5.94; found: C 57.79, H 4.93, N 5.72.

1-(2-(4-(Bis(4-methoxyphenyl)amino)phenoxy)ethyl)-1'-ethyl-[4,4'-bipyridine]-1,1'-dium tetrafluoroborate (TPA-Vio) (6). Compound **5** (1.07 g, 2.5 mmol) was dissolved in acetonitrile (60 mL) followed by addition of **1** (1.35 g, 5.0 mmol), and the resultant solution was stirred at reflux for 72 h. After reaction and filtration, the collected solid was dissolved in DI water and added to saturated NaBF₄ solution dropwise to form a precipitate. The precipitate was collected by filtration and dried under vacuum to obtain **6** as a pale purple powder (0.920 g, 60%). M.p.: 195–200 °C measured using a melting point system at 5 °C min⁻¹. ¹H NMR (400 MHz, DMSO-*d*₆, δ): 1.60 (t, 4H), 3.70 (s, 6H), 4.52 (t, 2H), 4.71–4.76 (m, 2H), 5.13 (t, 2H), 6.84 (m, 12 H), 8.79–8.83 (m, 4H), 9.41–9.45 (m, 4H); ¹³C NMR (100 MHz, DMSO-*d*₆, δ): 16.45, 55.39, 56.74, 60.34, 66.51, 114.93, 115.77, 123.91, 124.94, 126.59, 126.84, 141.22, 142.52, 145.69, 146.50, 148.71, 149.37, 152.57, 154.96; ESI-MS *m/z*: calcd for (C₃₄H₃₅N₃O₃)⁺, 533.27; found, 533.27. Anal. calcd for C₃₄H₃₅B₂F₈N₃O₃: C 57.74, H 4.99, N 5.94; found: C 57.79, H 4.93, N 5.72.

2-(4-(Bis(4-methoxyphenyl)amino)phenoxy)anthracene-9,10-dione (TPA-OAQ) (7). K₂CO₃ (5.53 g, 40 mmol) was dissolved in DMSO (50 mL), and 2-chloroanthraquinone (5.34 g, 22 mmol) and **4** (10.55 g, 20 mmol) were added successively at room temperature. The mixture was heated to 100 °C with stirring for 24 h and monitored by TLC. After cooling, the mixture was slowly poured into methanol/water (1 : 1). The precipitate was filtered, washed with hot methanol and dried over vacuum system to obtain **7** as a red powder (9.33 g, 84%). M.p.: 144–145 °C measured using a melting point system at 5 °C min⁻¹. ¹H NMR (400 MHz, DMSO-*d*₆, δ): 3.74 (s, 6H), 6.87 (d, 2H), 6.93 (d, 4H), 7.05–7.08 (m, 6H), 7.45–7.51 (m, 2H), 7.89–7.94 (m, 2H), 8.15–8.22 (m, 3H); ¹³C NMR (100 MHz, DMSO-*d*₆, δ): 55.22, 112.55, 115.01, 120.92, 121.48, 122.41, 126.53, 126.70, 127.53, 129.91, 132.98, 134.27, 134.66, 135.15, 140.14, 146.06, 147.03, 155.75, 163.11, 181.24, 182.08. ESI-MS *m/z*: calcd for (C₃₄H₂₅NO₅)⁺, 527.17; found, 527.18. Anal. calcd for C₃₄H₂₅NO₅: C 77.41, H 4.78, N 2.65; found: C 77.48, H 4.60, N 2.70.

Fabrication of electrochromic device

Two ITO glasses (~5 Ω □⁻¹) were laminated with thermosetting adhesives using a full-auto dispenser and heated at 150 °C for 2 h to obtain vacant devices with gaps of 120 μm (controlled by beaded glass dispersion in the adhesives), and the active areas of the devices were controlled at 2 cm × 2 cm. A tiny hole was left in one side of the device for the later injection of electrochromic liquid electrolyte. After electrolyte injection, for which the total amount of polypropylene carbonate inside the device, based on its

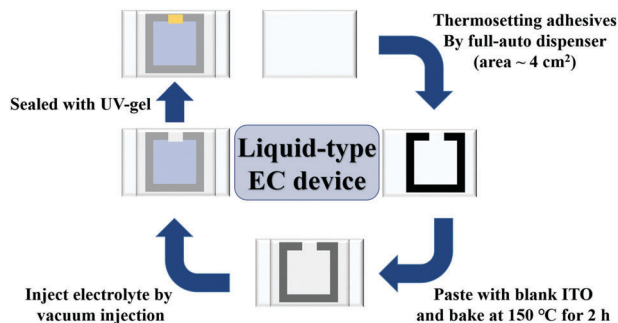


Fig. 1 Schematic diagram of fabrication process for ECDs based on liquid-type EC electrolyte.

vacant volume, was ~ 0.048 mL, the cells were eventually sealed completely with UV gel. The liquid-type electrolyte assembly was based on **TPA-3OMe** (0.015 M), **6** (0.030 M), and **7** (0.030 M), with 0.10 M TBABF₄ dissolved in propylene carbonate (PC). Fig. 1 shows the entire ECD fabrication process.

Results and discussion

Material synthesis

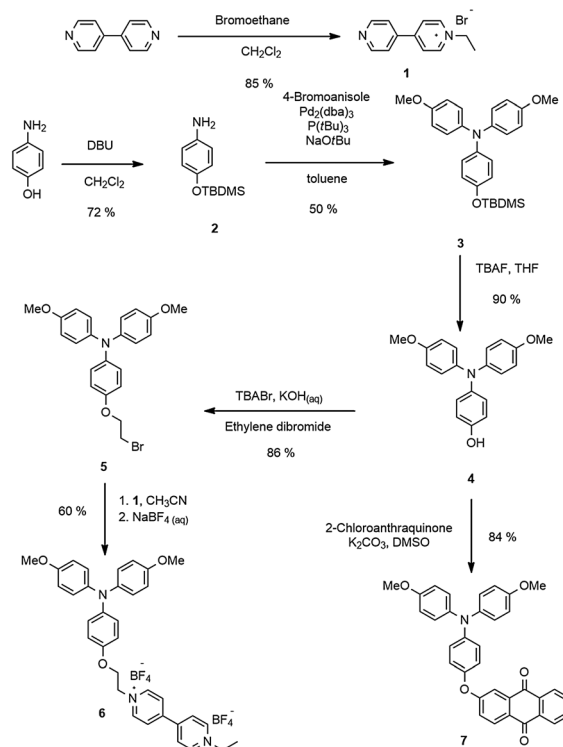
TPA-3OMe (m.p.: 92–93 °C using a melting point system at 5 °C min⁻¹; lit. 17, 90–92 °C) was obtained from the copper-catalyzed reaction of *p*-anisidine with 4-iodoanisole, and the result was in agreement with a previous study. **TPA-Vio** (**6**) was synthesized by the nucleophilic substitution reaction of **5** with **1**, affording a 60% yield. **TPA-OAQ** (**7**) was prepared by the potassium carbonate-mediated reaction of **4** with 2-chloroanthraquinone to give an 84% yield. NMR spectroscopy and elemental analysis were used to characterize the structures of intermediate **5** and final compounds **6** and **7**. Scheme 1 shows the entire synthetic procedure. The structures of the obtained intermediates and target compounds (**5–7**) were confirmed by NMR measurements, as summarized in Fig. S1–S9 (ESI[†]).

Electrochemistry

The electrochemical and EC behaviours of **TPA-3OMe**, **6**, and **7** were investigated by cyclic voltammetry (CV) measurements using a customized OTLE cell containing 10⁻³ M EC materials, anhydrous propylene carbonate (PC) as solvent, and 0.1 M TBABF₄ as the supporting electrolyte. Their CV diagrams are shown in Fig. 2, and the results of the respective half-wave redox potentials are summarized in Table 1. Compared to **TPA-3OMe**, the oxidation voltages of **6** and **7** were higher due to replacing a less electron-donating substituent. By incorporating the soft ether linkage segment, the cathodic EC moieties within **6** and **7** could be isolated and behaved independently. Furthermore, the redox potentials of anodic (TPA) and cathodic (viologen and anthraquinone units) EC functionalities seemed to match each other, which could be further confirmed in the ECDs by their switching behaviours.

Spectroelectrochemistry

Spectroelectrochemical measurements were conducted under the same conditions mentioned above using an OTLE cell



Scheme 1 Synthesis of ambipolar TPA derivatives **6** and **7**.

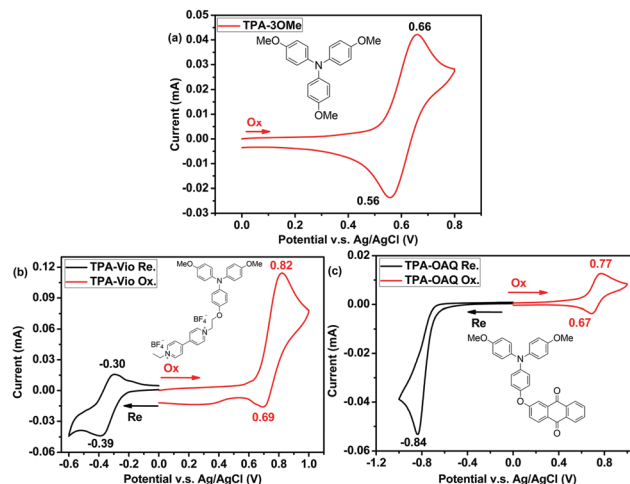


Fig. 2 CV diagrams for 0.001 M of (a) **TPA-3OMe**, (b) **6**, and (c) **7** in 0.1 M TBABF₄ PC solution at a scan rate of 50 mV s⁻¹ and using a platinum net as the working electrode.

built from a commercial UV-vis cuvette to demonstrate the EC behaviours of these materials. The results at different redox applied potentials are shown in Fig. 3.

Both **6** and **7** produced similar results to **TPA-3OMe** when 1.0 V was applied to the systems, with absorbances at 360 and 727 nm for **6** and 366 and 734 nm for **7**, corresponding to similar colour changes (from transparent to cyan during oxidation procedures). For cathodic EC behaviour, two new absorption peaks at 399 and 606 nm appeared for **6** when the potential increased

Table 1 Redox data of TPA-3OMe, **6**, and **7**

Material	Oxidation (vs. Ag/AgCl)		Reduction (vs. Ag/AgCl)	
	E_{onset}^a (V)	$E_{1/2}^b$ (V)	E_{onset}^a (V)	$E_{1/2}^b$ (V)
TPA-3OMe	0.53	0.61	—	—
6	0.67	0.76	-0.26	-0.35
7	0.65	0.73	-0.71	-0.84 ^c

^a Onset half-wave potentials were obtained from CV. ^b Half-wave potentials from cyclic voltammograms. ^c Reduction potentials from cyclic voltammograms.

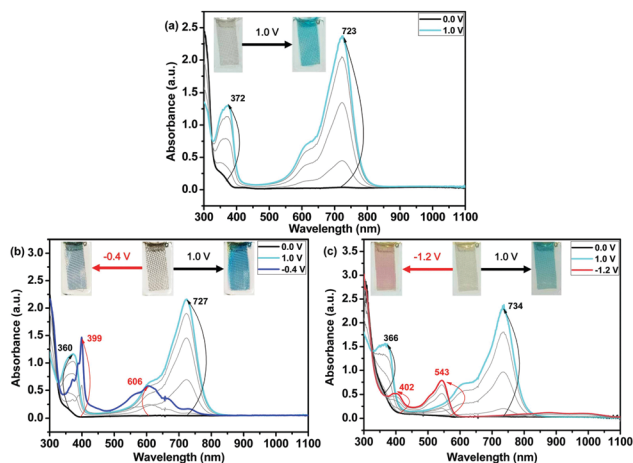


Fig. 3 Electrochromic behaviour and corresponding photographs of (a) TPA-3OMe, (b) **6**, and (c) **7** at the applied potentials from 0 to (a) 1.0, (b) 1.0, -0.4, and (c) 1.0, -1.2 V (vs. Ag/AgCl) based on 0.001 M of material in PC containing 0.1 M TBABF₄.

from 0 to -0.4 V owing to the formation of viologen cation radicals, resulting in a colour change from colourless for the original dication form to blue for the reduced state. For **7**, the absorption of two new peaks at 402 and 543 nm was observed and increased obviously from 0 to -1.2 V. The formation of a monoanion radical in the anthraquinone moiety switched the colour from almost colourless to pink. Furthermore, to obtain more insight into the EC behaviour of the ambipolar materials, two slices of ITO coated glass were used as working and auxiliary electrodes, respectively, to simulate the colouration mechanism in the device system. As an example, **6** exhibited reversible colouring and bleaching changes on both electrodes in the same amount of time at an applied potential of 0.8 V, as depicted and proposed in Fig. 4.

Electrochromic devices and properties

Moreover, ECDs derived from ambipolar EC materials **6** or **7** showed the same redox driving voltages to achieve the coloured stage, regardless of the different phases of applied voltage (Fig. 5a), and the working potential of **6** (1.2 V) was much lower than that of the device derived from TPA-3OMe (2.2 V; Fig. S10, ESI[†]). Furthermore, the incorporation of counter EC moieties reduced the driving voltage and caused the absorption of new peaks in visible-light region at 606 nm (viologen unit) and 724 nm (TPA unit) for **6** to gradually increase simultaneously. These could be merged together to reach high $\Delta T\%$ of 87% at 606 nm and 96% at 724 nm, as shown in Fig. 6a and b.

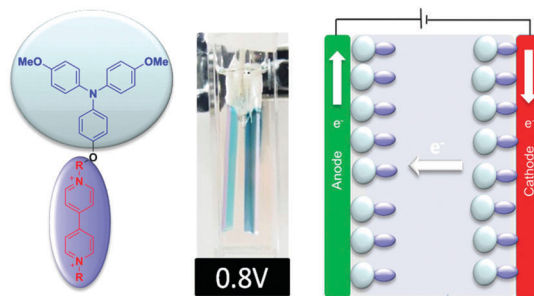


Fig. 4 Schematic diagram of colour change for ambipolar materials using **6** as a model in a quartz glass square at an applied potential of 0.8 V (vs. Ag/AgCl).

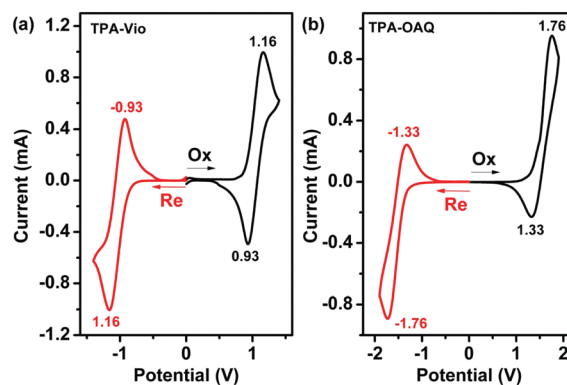


Fig. 5 CV diagrams of ECDs containing 0.03 M of (a) **6** and (b) **7** in 0.1 M TBABF₄/PC solution at a scan rate of 50 mV s⁻¹. One ITO glass served as the working electrode and the other served as the counter electrode and reference electrode simultaneously.

Therefore, two complementary colours (cyan and blue) could be merged together, resulting in a much deeper blue colour and higher ΔL^* (L^* , 91.38–40.09; a^* , 0.25–13.09; b^* , 0.28–52.54).

Similarly, the absorption intensities at 535 nm (anthraquinone unit) and 734 nm (TPA unit) could increase simultaneously at a higher applied voltage of 1.8 V in the device based on ambipolar material **7**, and could combine two complementary colours (cyan and pink) with $\Delta T\%$ of 68% at 535 nm and 91% at 734 nm to produce a deeper violet colour (L^* , 68.51; a^* , 2.50; b^* , -11.36) of the device, as shown in Fig. 6c and d. As the potential voltage was turned to 0 V, both devices were easily bleached back to their original states. This outcome could be partly responsible for the viologen/anthraquinone moieties possessing the ability to induce electrons lost from the TPA moiety during the oxidative process, while the resultant monocation radical viologen and monoanion radical anthraquinone could also facilitate giving electrons back to monocation TPA during the reductive process.

According to the switching investigation of ECDs based on individual ambipolar EC materials, the results are summarized in Fig. 7. As depicted in Fig. 7a and b, the switching time of the ECD derived from **6** was 1.7 s and 2.7 s at 1.2 V for the colouring process at 724 nm (TPA moiety) and 606 nm (viologen moiety), and 9.7 s and 9.5 s, respectively, for the bleaching process without applied voltage.

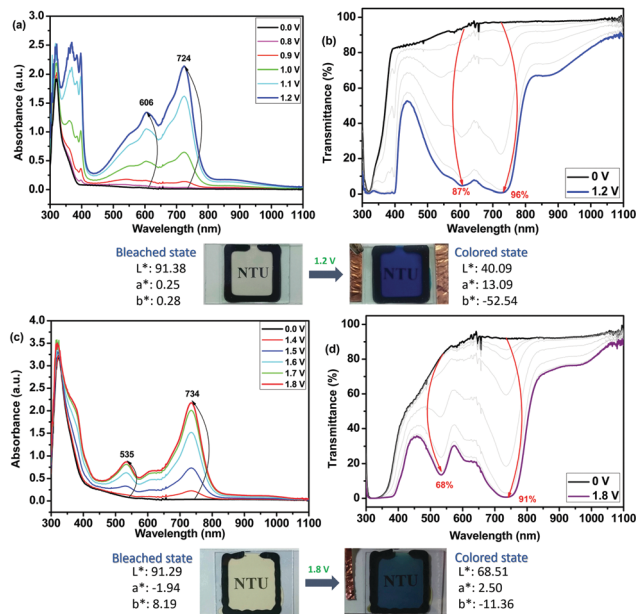


Fig. 6 (a) Absorbance spectrum and (b) transmittance spectrum of ECD based on **6** at an applied potential of 0 to 1.2 V and its corresponding photograph. (c) Absorbance and (d) transmittance spectra of ECD based on **7** at an applied potential of 0 to 1.8 V and its corresponding photograph.

The other device based on **7**, as shown in Fig. 6d and e, required 5.5 s for colouration at 535 nm and 5.3 s for decolouration of the anthraquinone moiety, and 3.2 s for colouration at 734 nm and 5.2 s for decolouration of the TPA moiety without applied voltage.

Notably, the results summarized in Table S1 (ESI[†]) show that the colouration of ECDs with ambipolar materials proceeded faster than the corresponding ECD based on **TPA-3OMe** EC material with only with an anodic EC unit. This was due to the connecting charge trapping moieties in **6** and **7** being able to effectively induce electron gain and loss. The amounts of injected charge (Q_{in}) obtained from Fig. 7c and f were 14.012 and 14.134 mC cm^{-2} for the colouring process of devices with **6** and **7**, respectively. According to the results described above, such devices demonstrated enhanced performance compared to the device with **TPA-3OMe** (Fig. S11a, ESI[†]).

As shown in Fig. 8, the electrochemical stabilities of the ECDs based on **6** and **7** were determined by evaluating the electrochromic CE ($\eta = \Delta OD/Q$) and injected charge (electroactivity) at various switching cycles, with the results summarized in Tables S2 and S3 (ESI[†]), respectively. After 1000 scanning cycles, the ECDs derived from **6** and **7** ambipolar EC materials maintained high reversibility and electroactivity without significant decay, while the ECD derived from **TPA-3OMe** exhibited much worse electrochemical stability for only 20 cycles (Fig. S11c, ESI[†]), probably owing to the much higher switching potential and lack of complementary cathodic EC moieties. The CE of the ECD fabricated from **6** reached 112 and 177 $\text{cm}^2 \text{C}^{-1}$ at 606 and 724 nm, and retained reversibility, with decays of 7 and 6%, respectively, after 1000 cycles between 0 and 1.2 V. In contrast, the CE of the ECD prepared from **7** showed CEs of 72 and 162 $\text{cm}^2 \text{C}^{-1}$ at 535 and

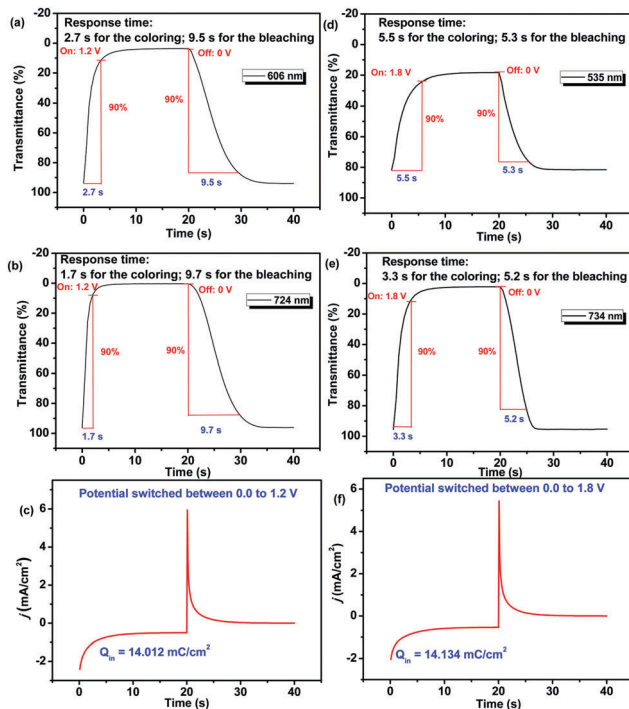


Fig. 7 Transmittance changes at (a) 724 nm and (b) 606 nm, and (c) chronoamperometry curve, of device containing **6** between 0 and 1.2 V. Transmittance changes at (d) 535 nm and (e) 734 nm, and (f) chronoamperometry curve, of device containing **7** between 0 and 1.8 V.

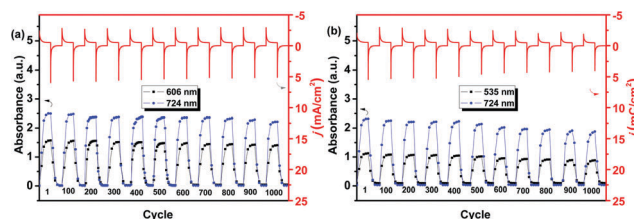


Fig. 8 Chronoamperometry curves and corresponding *in situ* absorbance at respective wavelengths of ECDs with (a) **6** between 0 and 1.2 V, and (b) **7** between 0 and 1.8 V.

734 nm, respectively, with decays of 10 and 5% after 1000 cycles. These outcomes were in agreement with the assumption that the incorporation of counter EC moieties into the TPA unit could effectively improve switching response time and enhance electrochemical stability.

Conclusions

High-performance ECDs of ambipolar EC materials **TPA-Vio** (**6**) and **TPA-OAQ** (**7**) have been fabricated successfully and investigated in spectroelectrochemical and EC switching studies. By incorporating cathodic EC moieties into TPA as a charge trapping layer, the resultant ambipolar ECDs not only reduced the driving voltage and switching time in the EC procedure compared with the devices using TPA only, but also showed the ability to merge the colours contributed by the anodic TPA and

cathodic EC moieties. This enhanced the electrochemical stability and EC performance of the obtained ECDs containing ambipolar EC materials. These results demonstrated conclusively that the incorporation of suitable counter EC moieties into TPA derivatives is a facile and feasible approach to fabricating novel ECDs.

Conflicts of interest

There are no conflicts to declare.

Acknowledgements

The authors gratefully acknowledge the Ministry of Science and Technology of Taiwan for the financial support.

Notes and references

- 1 R. J. Mortimer, D. R. Rosseinsky and P. M. S. Monk, *Electrochromic Materials Devices*, Wiley-VCH Verlag GmbH & Co. KGaA, Weinheim, Germany, 2015, pp. 1–210.
- 2 D. R. Rosseinsky and R. J. Mortimer, *Adv. Mater.*, 2001, **13**, 783–793.
- 3 T. Kuorosawa, C. C. Chueh, C. L. Liu, T. Higashihara, M. Ueda and W. C. Chen, *Macromolecules*, 2010, **43**, 1236–1244.
- 4 Y. Shirota and H. Kageyama, *Chem. Rev.*, 2007, **107**, 953–1010.
- 5 H. J. Yen and G. S. Liou, *Polym. Chem.*, 2012, **3**, 255–264.
- 6 H. J. Yen, H. Y. Lin and G. S. Liou, *Chem. Mater.*, 2011, **23**, 1874–1882.
- 7 R. J. Mortimer, *Electrochim. Acta*, 1999, **44**, 2971–2981.
- 8 A. Kavanagh, K. J. Fraser, R. Byrne and D. Diamond, *ACS Appl. Mater. Interfaces*, 2013, **5**, 55–62.
- 9 D. Weng, Y. C. Shi, J. M. Zheng and C. Y. Xu, *Org. Electron.*, 2016, **34**, 139–145.
- 10 C. L. Bird and A. T. Kuhn, *Chem. Soc. Rev.*, 1981, **10**, 49–82.
- 11 H. M. Wang and S. H. Hsiao, *J. Mater. Chem. C*, 2014, **2**, 1553–1564.
- 12 H. J. Yen, C. L. Tsai, S. H. Chen and G. S. Liou, *Macromol. Rapid Commun.*, 2017, **38**, 1600715.
- 13 S. H. Hsiao and J. Y. Lin, *J. Polym. Sci., Polym. Chem. Ed.*, 2016, **54**, 644–655.
- 14 H. J. Yen, K. Y. Lin and G. S. Liou, *J. Polym. Sci., Polym. Chem. Ed.*, 2012, **50**, 61–69.
- 15 Y. Ling, C. L. Xiang and G. Zhou, *J. Mater. Chem. C*, 2017, **5**, 290–300.
- 16 H. W. Chang, K. H. Lin, C. C. Chueh, G. S. Liou and W.-C. Chen, *J. Polym. Sci., Polym. Chem. Ed.*, 2009, **47**, 4037–4050.
- 17 G. Lamanna, C. Faggi, F. Gasparrini, A. Ciogli, C. Villani, P. L. Stephens, F. L. Devlin and S. Menichetti, *Chem. – Eur. J.*, 2008, **14**, 5747–5750.